Tumors induce *de novo* steroid biosynthesis in T cells to evade immunity

Bidesh Mahata[1, 2*], Jhuma Pramanik[1], Louise van der Weyden[1], Gozde Kar[2], Angela Riedel[3], Nuno A. Fonseca[2], Kousik Kundu[1], Edward Ryder[1], Graham Duddy[1], Izabela Walczak[1, 4], Sarah Davidson[3], Klaus Okkenhaug[5], David J. Adams[1], Jacqueline D. Shields[3*] and Sarah A. Teichmann[1, 6*]

1. Wellcome Sanger Institute, Wellcome Genome Campus, Hinxton, Cambridge, CB10 1SA, United Kingdom

2. EMBL-European Bioinformatics Institute, Wellcome Genome Campus, Hinxton, Cambridge, CB10 1SD, United Kingdom

3. Medical Research Council Cancer Unit, Hutchison/Medical Research Council Research Centre, Cambridge, UK

4. Iontas Ltd, Iconix Park, Cambridge, CB22 3EG, UK

5. Division of Immunology, Department of Pathology, University of Cambridge, Cambridge, CB2 1QP UK

6. Theory of Condensed Matter, Cavendish Laboratory, 19 JJ Thomson Ave, Cambridge, CB3 0HE, United Kingdom.

*To whom correspondence should be addressed: st9@sanger.ac.uk, JS970@mrc-cu.cam.ac.uk and bm11@sanger.ac.uk

Summary:

Tumors subvert immune cell function to evade immune responses[1], and the mechanisms of tumor immune evasion are incompletely understood. Here we show that tumors induce *de novo* steroidogenesis in T lymphocytes to evade anti-tumor immunity. Using a novel transgenic fluorescent reporter mouse line we identify and characterize *de novo* steroidogenic T cells. Genetic ablation of T cell steroidogenesis restricts primary tumor growth and metastatic dissemination in mouse models. Steroidogenic T cells dysregulate anti-tumor immunity, which can be restored by inhibiting the steroidogenesis pathway. This study demonstrates that T cell *de novo* steroidogenesis is a cause of anti-tumor immunosuppression and a druggable target.

Steroidogenesis is a metabolic process by which cholesterol is converted to steroids[2]. The biosynthesis of steroids starting from cholesterol is often termed "*de novo* steroidogenesis"[1]. Cytoplasmic cholesterol is transported into the mitochondria, where the rate-limiting enzyme CYP11A1 (also known as P450 side chain cleavage enzyme) converts cholesterol to pregnenolone. Pregnenolone is the first bioactive steroid of the pathway, and the precursor of all other steroids (Figure 1a) [2,3]. The steroidogenesis pathway has been extensively studied in adrenal gland, gonads and placenta. *De novo* steroidogenesis by other tissues, known as "extraglandular steroidogenesis", in brain[2,4,5], skin[6], thymus[7], and adipose tissues[8] has also been reported. Steroid production as a result of immune induction from mucosal tissues, such as in the lung and intestine, has been shown to play a tolerogenic role to maintain tissue homeostasis[9,10]. However the physiological and pathological role of extraglandular steroidogenesis is largely unknown[3].

Steroid hormones are known immunosuppressive biomolecules[11,12]. We recently reported that $CD4^+$ T cells induce *de novo* steroidogenesis to restore immune homeostasis by limiting the immune response against a worm parasite[13]. In cancer, the immunosuppressive tumor microenviroenmnt (TME) prevents immune cells from mounting an effective anti-tumor immune reposne[1]. Thus we sought to determine whether T cell steroidogenesis contributes to the generation of a suppressive niche in the TME.

Cyp11a1 expression is known to be a faithful biomarker of *de novo* steroidogenesis due to its role as a central enzyme in this pathway[2]. Therefore, we generated a novel reporter mouse line to identify Cyp11a1-expressing steroidogenic cells definitively (Figure 1b, c, Extended Data Figure 1a, b, c and d). As expected, mCherry expression was detected in single cell suspensions of testis and adrenal glands but not in the spleen (Figure 1c) or other tissues including lung, kidney, blood, liver, bone marrow, lymph nodes and thymocytes (Extended Data Figure 1b).

However, upon activation *in vitro,* Cyp11a1-mCherry signal was detected specifically in activated type-2 $CD4^+$ T helper cells (Th2 cells) (Extended Data Figure 1c), as reported previously[13]. Cyp11a1 expression was only detectable in mCherry-expressing T helper cells but not in the mCherry-negative T helper cells (Extended Data Figure 1d). Exploiting our *Cyp11a1*-mCherry reporter line, we assayed a panel of cytokines commonly found in inflammatory settings, including tumors, in terms of their ability to induce steroidogenesis in $CD4^+$ T cells. IL6, TSLP, IL13, and IL4 induced a strong induction of Cyp11a1-mCherry in $CD4^+$ T cells that had also been

activated by anti-CD3 and anti-CD28. In contrast, IL12 had minimal effect on steroidogenesis (Figure 1d, Extended Data Figure 2a and b). This result indicates that not only the Th2 but also other T cell types are capable of *de novo* steroidogenesis. To test this, we differentiated naïve $CD4^+$ or $CD8^+$ T cells into Th1, Th2, Th9, Th17, Tfh, Treg, Tc1 and Tc2 subsets *in vitro*. All subsets examined, with the exception of Th1 and Tc1 exhibited *Cyp11a1*-mCherry expression when stimulated (Figure 1e, Extended Data Figure 2c). Of all T cell subtypes generated *in vitro*, Th2 cells exhibited the highest levels of Cyp11a1 expression.

Tumor infiltrating T cells are key fate determinants within a tumor, but are often suppressed[14]. The steroidogenesis-inducing cytokines examined above are also often present in the TME[15,16], thus we next sought to examine the steroidogenic capacity of T cells infiltrating tumors, and their impact on tumor development. First, to explore Cyp11a1 expression *in vivo,* we utilized the well-established B16-F10 melanoma model[17-19] and generated subcutaneously implanted tumors in *Cyp11a1*-mCherry reporter mice.

Cyp11a1 expression was detected in immune cells of primary tumor tissue, but not in tumor-draining brachial lymph nodes (LN) or blood (Figure 2a), indicating that stimulation occurs *in situ*. Within the tumor, $Cyp11a1^+$ tumor infiltrating T cells were predominantly $CD4^+$ (helper T cells) rather than $CD8^+$ T cells (Figure 2b). We next measured the functional output of Cyp11a1 expression. Significant concentrations of the steroid pregnenolone were detected exclusively in immune cells isolated from tumors, with negligible levels detected in cells from the spleen (Figure 2c). Using the B16-F10 model of experimental metastatic dissemination[20], we determined that lungs

with metastatic nodules, but not control lungs without metastatic nodules, had elevated levels of pregnenolone (Figure 2d).

Having observed steroidogenic T cells in murine melanoma, we turned to publicly available transcriptomic data sets to verify our findings and ascertain relevance in the human setting. We identified *CYP11A1* mRNA expression, and thus steroidogenic potential, in a range of cancer types including liver, breast, prostate, lung, kidney, sarcoma, glioma, uterine, cervical, lymphoma and melanoma (Figure 2e and Extended Data Figure 3a,b)[16]. Human melanoma tissues represented a prominent steroidogenic tumor type, expressing *CYP11A1, HSD3B1, HSD3B2, CYP17A1, CYP21A1, CYP11B1* (Figure 2f). Together, this was indicative of melanoma-driven production of glucocorticoids (Figure 2f, Extended Data Figure 3c).

Interestingly, in melanoma, steroidogenic gene expression was correlated with *IL4* expression (Figure 2f, Extended Data Figure 3d), a key inducer of T cell steroidogenesis. Moreover, analysis of human tumor infiltrating $CD4^+$ T cell transcriptomes, confirmed *CYP11A1* expression (Figure 2g) implying that $CD4^+$ T cells are a source of steroids in tumors, mirroring the murine setting. Collectively these data indicate that TILs produce steroids within the tumor both in human and mouse. Since steroid hormones are efficient modulators of metabolism and potent regulators of immune cell function, it is plausible that T cell-mediated steroid biosynthesis may have a profound effect on tumor growth and metastasis.

To determine the functional consequences of T cell-driven steroidogenesis in tumors, we created a *Cyp11a1* floxed (*Cyp11a1*$^{fl/fl}$) mouse following EUCOMM/WSI

conditional gene targeting strategy[21]. Briefly, a "Knockout-first" (*tm1a*) mouse line was created using a promoter-driven targeting cassette (Figure 3a). The *tm1a* mouse was then crossed with Flp-deleter mice (FlpO) [22] to remove the *LacZ* and *Neo* cassette and generate a *tm1c* allele (i.e. *Cyp11a1*$^{fl/fl}$). When crossed with a Cre-driver, the Cre-recombinase removes exon 3 of *Cyp11a1* gene and creates a frameshift mutation (Figure 3a). We crossed the *Cyp11a1*$^{fl/fl}$ line with a *Cd4*-driven Cre-recombinase to delete *Cyp11a1* and prevent *de novo* steroidogenesis in all T cells. Deletion efficiency of Cre-recombinase in the *Cyp11a1* cKO (*Cd4-Cre;Cyp11a1*$^{fl/fl}$) mice was nearly 100% in Th2 cells (Extended Data Figure 4a). *Cyp11a1* cKO mice showed normal thymic development of T cells, and a normal distribution in the peripheral tissues (Extended Data Figure 4b, c).

We subcutaneously implanted *Cyp11a1* cKO mice with B16-F10 cells to explore the pathophysiological role of T cell steroidogenesis. Ablation of steroidogenesis in T cells significantly restricted primary tumor growth rates and final volumes (Figure 3b). Similarly, in the experimental metastatic dissemination model, impaired lung colonization was observed in the absence of T cell-expressed Cyp11a1: there was a significant reduction in number of lung metastatic foci in the *Cyp11a1* cKO mice compared to the control mice (Figure 3c).

In the B16-F10 subcutaneous melanoma model, topical application of pregnenolone at the primary tumor site was sufficient to compensate for the Cyp11a1 deficiency, restoring tumor growth to levels comparable with control mice (Figure 3d). Furthermore, pharmacological inhibition of Cyp11a1 by aminoglutethimide (AG)

recapitulated the tumor restriction phenotype of *Cyp11a1* genetic deletion (Figure 3e). Together, these data indicate that, T cell-derived steroids can support tumor growth.

It has been reported that steroid hormones induce immunosuppressive M2 phenotype in macrophages[11,23], cell death and anergy in T cells[11] and tolerance in dendritic cells[11 24]. Therefore we set out to test whether steroidogenic T cells support tumor growth through the induction of immunosuppressive phenotypes in infiltrating immune cells. To determine whether intratumoral macrophages were M1 or M2 type, we purified tumor infiltrating macrophages ($Lin^{-}CD45^{+}CD11b^{+}$) and analyzed mRNA expression of the M2-macrophage signature genes *Arg1* and *Tgfb1*. In tumor-infiltrating macrophages from *Cyp11a1* cKO mice, *Arg1* and *Tgfb1* mRNA expression was significantly reduced compared to the control mice, indicating fewer of the tumour-supporting M2 macrophages in the knockout mice (Figure 4a).

Conversely, significantly higher levels of the cytokines *Ifng* and *Tnfa* expression were identified in tumor infiltrating $CD8^{+}$ T cells (Figure 4b). Examination of co-inhibitory receptors Tim-3, PD-1, TIGIT and Lag3[25-27] on tumor-infiltrating T cells revealed a significant reduction in the frequency of PD1 and TIGIT expressing $CD8^{+}$ TILs in the *Cyp11a1* cKO mice compared with control littermates. This indicates greater T cell functionality and less exhaustion in the knockout mice (Figure 4c).

To test the tumor cell killing cytotoxic nature of T and NK cell populations, we examined the degranulation response of these cells by analyzing cell surface expression of CD107a/LAMP1 in tumor-infiltrating T and NK cells. We observed a significantly increased proportion of degranulating $CD107a^{+}CD8^{+}$ T cells in *Cyp11a1*

cKO mice compared to control mice (Figure 4d). There was trend for enhanced degranulation response in NK cells and $CD4^+$ T cells (Figure 4e, f). Altogether these data suggest that inhibition of T cell steroidogenesis boosts active and functional anti-tumor immunity.

The importance of systemic steroid hormones is well documented in regulating cell metabolism and immune cell function in homeostasis, but the role of local cell type specific steroidogenesis is less clear, particularly in pathologies such as cancer. This is in part due to the lack of tools to study steroidogenesis in a tissue-specific manner *in vivo*. To overcome this, we generated a novel *Cyp11a1*-mCherry reporter and a conditional *Cyp11a1* knockout mouse strain to identify *de novo* steroidogenic cells and study their role *in vivo*.

Using these discovery tools, we uncovered a novel anti-tumor immune suppression mechanism that may be exploited clinically to boost the anti-tumor immunity (Figure 4g). Similar experimental approaches can in future provide in depth mechanistic insights into other extraglandular (local) steroidogenic cell types such as adipose cells, neuron, osteoblasts, astrocytes, microglia, skin, trophoblast and thymic epithelial cells. Furthermore, our *Cyp11a1*-mCherry reporter mouse line can be used as a discovery tool to identify new steroidogenic cell types in tolerogenic physiological conditions such as pregnancy, mucosal tolerance, and inflammatory and immunopathological conditions such as virus, bacteria, fungi and parasite infections. Their functional role can be dissected by using *Cyp11a1* cKO mice using tissue specific Cre-drivers.

Finally, the ability of several cytokines (including IL4, IL5, IL13, IL33, IL23, TSLP, and IL6) to induce steroidogenesis in T cells opens up the possibility that this mechanism is involved in numerous immunological contexts. Further studies in diverse physiological scenarios would be of great interest to more broadly understand the role of immune cell *de novo* steroidogenesis in regulating inflammation and immunity.

Materials and Methods

Mice

The care and use of all mice in this study were in accordance with the UK Animals in Science Regulation Unit's Code of Practice for the Housing and Care of Animals Bred, Supplied or Used for Scientific Purposes, the Animals (Scientific Procedures) Act 1986 Amendment Regulations 2012. All procedures were performed under a UK Home Office Project licence (PPL 80/2574 or PPL P8837835), which was reviewed and approved by the local institute's Animal Welfare and Ethical Review Body.

Generation of a Cyp11a1-mCherry reporter mouse line

Targeting Description: Using CRISPR_Cas9 (Clustered Regularly Interspaced Short Palindromic Repeats) [28] technology we introduced double strand DNA breaks 5' and 3' adjacent to the *Cyp11a1* termination codon in exon 9 to facilitate the introduction of our targeting construct. The 5' and 3' arms of homology were designed to remove the *Cyp11a1* termination codon and 100bp of the 3' UTR immediately downstream and replace it with a minimal T2a self-cleavage peptide followed by the fluorescent marker mCherry.

Cyp11a1 Guide RNA generation and ESC targeting.

sgRNA design and cloning: Using the web-based tool designed by Hodgkins et al[29], two sgRNAs were identified 5' and 3' adjacent to the Cyp11a1 termination codon. The guide sequences were ordered from Sigma Genosys as sense and antisense oligonucleotides, and annealed before individually cloning into the human U6 (hU6) expression plasmid (kind gift from Sebastian Gerety).

Targeted ES cell generation: $3x10^{6}$ C57Bl/6 JM8 ESC (kind gift from Bill Skarnes) were nucleofected with 2ugs *Cyp11a1* circular targeting construct, 1.5ugs of each hU6_sgRNAs and 3ugs a plasmid expressing human codon-optimised CAS9 driven by the CMV promotor (Addgene # 41815). 48 hours post transfection the media was changed for G418 selection media. Confirmation of the correct targeting events were confirmed by qPCR for loss of heterozygosity (LOH) and the presence of the selectable marker, and long range (LR) PCR and Sanger sequencing.

Breeding and removal of the Selectable marker: Following blastocyst injection and chimaera breeding three F1 $Cyp11a1^{+/mCherry\text{-}Neo}$ (MGWG18.1f, MGWG16.1b, MGWG16.1d) mice were breed to pCAGGSs-Flpo (kind gift from Andrea Kranz)[22] mice to remove the neomycin selectable marker to generate $Cyp11a1^{+/mCherry}$.

Generation of a Cyp11a1 cKO mice

$Cyp11a1^{fl/fl}$ mice were generated by crossing $Cyp11a1^{tm1a(KOMP)Wtsi}$ mice with a previously reported Flp-deleter (FlpO) line[22]. *$Cyp11a1^{fl/fl}$* mice were crossed with *Cd4-cre* mice to generate the *Cyp11a1* cKO mice.

Syngeneic melanoma model

The C57BL/6 derived B16-F10 melanoma cell line was purchased from American Type Culture Collection (ATCC) and cultured in Dulbecco's Modified Eagle medium (DMEM, Life Technologies), supplemented with 1% Penstrep and 10% FBS. For the primary tumor growth assay, 2.5 x10^5 B16-F10 cells were injected subcutaneously into the shoulders of either wild type (WT) C57BL/6 mice, *Cd4-Cre, Cyp11a1*$^{fl/fl}$ or *Cd4-Cre;Cyp11a1*$^{fl/fl}$ mice. After 5, 8 and 11 days animals were sacrificed and tissues collected for analysis. In addition, skin was also taken from non-tumor bearing mice. For the experimental metastasis assay, 5×10^5 B16-F10 cells in a volume of 0.1 ml PBS were injected intra-venously into the tail vein. After ten days (±1 day) the mice were sacrificed *via* cervical dislocation, and their lungs removed and rinsed in phosphate buffered saline. The number of B16-F10 colonies on all five lobes of the lung were counted macroscopically.

Tumor Tissue Processing

Tumors were mechanically dissociated and digested in 1mg/ml collagenase D (Roche), 1mg/ml collagenase A (Roche) and 0.4mg/ml DNase (Roche) in PBS, at 37°C for 2 hrs. Lymph nodes were mechanically dissociated and digested with 1mg/ml collagenase A (Roche) and 0.4mg/ml DNase (Roche) in PBS, at 37^{0}C for 30 mins, after which time, Collagenase D (Roche) was added (final concentration of 1mg/ml) to lymph node samples and digestion was continued for a further 30 mins. EDTA was added to all samples to neutralize collagenase activity (final concentration (5mM) and digested tissues were passed through 70μm filters (Falcon).

Cell sorting

Once processed, single cell suspension tumour samples were incubated with a fixable fluorescent viability stain (Life Technologies) for 20mins (diluted 1:1000 in PBS) prior to incubation with conjugated primary antibodies for 30 mins at 4^0C. Antibodies were diluted in PBS 0.5% BSA. Stained samples were sorted, using the MoFlo XDP or BD Influx cytometer system.

T helper Cell Culture

Splenic naïve T helper cells from *Cyp11a1*-mCherry reporter mice were purified with the $CD4^+CD62L^+$T Cell Isolation Kit II (Miltenyi Biotec) and polarized *in vitro* toward differentiated Th1, Th2, Th9, Th17, iTreg and Tfh subtype as described previously (Pramanik J et al, 2018)[30]. In brief, naïve cells were seeded into anti-CD3e (2 µg/ml, clone 145-2C11, eBioscience) and anti-CD28 (5 µg/ml, clone 37.51, eBioscience) coated plates. The medium contained the following cytokines and/or antibodies:

Th1 subtype: Recombinant murine IL2 (10 ng/ml, R&D Systems), recombinant murine IL12 (10 ng/ml, R&D Systems) and neutralizing anti-IL4 (10µg/ml, clone 11B11, eBioscience). *Th2 subtype:* Recombinant murine IL2 (10 ng/ml, R&D Systems), recombinant murine IL-4 (10 ng/ml, R&D Systems) and neutralizing anti-IFNg (10µg/ml, clone XMG1.2, eBioscience). *Th9 subtype:* 20ng/ml recombinant mouse IL4, 2ng/ml recombinant human TGFb, 10µg/ml neutralizing anti-IFNg. *Th17 subtype:* 30ng/ml recombinant mouse IL6, 5ng/ml recombinant human TGFb, 50ng/ml recombinant mouse IL23. *Tfh subtype:* 50ng/ml recombinant mouse IL21, 10µg/ml neutralizing anti-IL4 and anti-IFNg. *iTreg subtype*: 5ng/ml recombinant mouse IL2, 5ng/ml recombinant human TGFb. The cells were removed from the activation plate on day 4 (after 72 hrs). Th2 cells were cultured for another two days

in the absence of CD3e and CD28 stimulation. Then, cells were restimulated by seeding on coated plate for 6 hrs. For flow cytometric detection cells were treated with monensin (2μM, eBioscience) for the last 3 hrs.

In vitro Tc1 and Tc2 differentiation

Splenic naïve $CD8^+$ T cells were purified by using Naive $CD8a^+$ T Cell Isolation Kit, mouse (Miltenyi Biotec) following manufacturers protocol, and polarized *in vitro* toward differentiated Tc1 and Tc2. In brief, naive cells were seeded into anti-CD3e (2 μg/ml, clone 145-2C11, eBioscience) and anti-CD28 (5 μg/ml, clone 37.51, eBioscience) coated plates. The medium contained the following cytokines and/or antibodies:

Tc1 subtype: Recombinant murine IL2 (10 ng/ml, R&D Systems), recombinant murine IL12 (10 ng/ml, R&D Systems) and neutralizing anti-IL4 (10μg/ml, clone 11B11, eBioscience). *Tc2 subtype:* Recombinant murine IL2 (10 ng/ml, R&D Systems), recombinant murine IL-4 (10 ng/ml, R&D Systems) and neutralizing anti-IFNg (10μg/ml, clone XMG1.2, eBioscience).

Quantitative PCR (qPCR)

Tumor infiltrating macrophages (Lin^-CD11b^+) and $CD8^+$ T cells were purified by cell sorting. We used the Cells-to-C_T kit (Invitrogen/Thermofisher Scientific) and followed SYBR Green format according to manufacturers instructions. 2μl of cDNA was used in 12μl qPCR reactions with appropriate primers and SYBR Green PCR Master Mix (Applied Biosystems). Data were analyzed by ddCT method. Experiments were performed 3 times and data represent mean values ± standard deviation. The primer list is provided below:

Arg1: F- ATGGAAGAGACCTTCAGCTAC

R- GCTGTCTTCCCAAGAGTTGGG

Tgfβ1: F- TGACGTCACTGGAGTTGTACGG

R- GGTTCATGTCATGGATGGTGC

Ifnγ: F- ACAATGAACGCTACACACTGC

R- CTTCCACATCTATGCCACTTGAG;

Tnfα: F- CATCTTCTCAAAATTCGAGTGACAA

R- TGGGAGTAGACAAGGTACAACCC

Gapdh: F- ACCACAGTCCATGCCATCAC

R- GCCTGCTTCACCACCTTC

Rplp0: F: CACTGGTCTAGGACCCGAGAA

R: GGTGCCTCTGGAGATTTTCG

Flow cytometry

We followed eBioscience surface staining, intracellular cytotoplasmic protein staining (for cytokines) and intracellular nuclear protein staining (for transcription factors and Cyp11a1) protocols. Briefly, single cell suspension was stained with Live/Dead Fixable Dead cell stain kit (Molecular Probes/ Thermo Fisher) and blocked by purified rat anti-mouse CD16/CD32 purchased from BD Bioscience and eBioscience. Surface staining was performed in flow cytometry staining buffer (eBioscience) or in PBS containing 3% FCS at 4^0C. For intracellular cytokine staining cells were fixed by eBioscience IC Fixation buffer and permeabililzed by eBioscience permeabilization buffer. For intra-organelle staining (nuclear and mitochondrial proteins) cells were fixed and permeabilized using Foxp3/Transcription Factor Fixation/Permeabilization Concentrate and Diluent (eBioscience) following the manufacturer's protocol. Cells were stained in 1x permeabilization buffer with fluorescent dye-conjugated

antibodies. After staining cells were washed with flow cytometry staining buffer (eBioscience) or 3% PBS-FCS, and were analyzed by flow cytometer Fortessa (BD Biosciences) using FACSDiva. The data were analyzed by FlowJo software. Antibodies used in flow cytometry were: CD4 (RM4-5 or GK1.5), CD8a (53-6.7), CD3e (145-2c11), CD45 (30F11), CD44 (IM7), CD25 (PC61), B220 (Ra3-6b2), Cyp11a1 (C-16, unconjugated, Santa Cruz; Fluorescent dye conjugated anti-goat secondary was used for staining), Ly6G (1A8), Ly6G/Ly6C (Gr-1) (RB6-8C5), Ly6C (HK1.4), CD11b (M1/70), CD11c (N418), CD19 (1D3), NK1.1(Pk136), Ter119 (TER119), PD-1 (J43), TIGIT (1G9), CD107a/LAMP1(1D4B). All antibodies were purchased from eBioscience, BD Bioscience or Biolegend.

Western Blot Antibodies

Anti-CYP11A1 (Santa Cruz Biotechnology, C-16) and anti-TBP (Abcam) were used.

Quantitative ELISA

$CD45^+$ leukocytes were purified from B16-F10 tumor masses and lungs, of mice that had been tail vein administered B16-F0 cells, and seeded at equal density in IMDM medium supplemented with 10% charcoal stripped fetal bovine serum (Life Technologies, Invitrogen) for 24 hrs. Pregnenolone concentrations of the culture supernatants were quantified using pregnenolone ELISA kit (Abnova) and corticosteroids ELISA (Thermofisher) kit following manufacturers' instruction. Absorbance was measured at 450 nm, and data were analyzed in GraphPad Prism 5.

Acknowledgements

We would like to thank Ana C. Anderson and Rahul Roychoudhuri for their valuable comments on the manuscript and useful discussions; Jana Eliasova for her help with diagram illustration; Bee Ling Ng, Chris Hall, Sam Thompson and Jennie Graham for help with flow cytometry and cell sorting; Research Support Facility, WSI, for their technical help and animal husbandry.

Funding

CRUK Cancer Immunology fund (Ref. 20193), ERC consolidator grant (ThDEFINE, Project ID: 646794) and Wellcome Sanger Institute core funding (WT206194) supported this study.

Author contribution

BM: Led and managed the project, generated hypothesis, designed and performed experiments, analyzed data. JP: Performed experiments, analyzed data and helped in genetically modified mouse generation. LvdW: Performed B16-F10 pulmonary metastasis experiments, analyzed data. AR: Performed B16-F10 subcutaneous tumors experiments, analyzed data. GK, NAF and KK: Analyzed publicly available gene expression datasets to confirm human tumor expression of steroidogenic genes. ER and GD: Helped in generation of *Cyp11a*-mCherry and *Cyp111a1*$^{fl/fl}$ mouse model. IW: Built the *Cyp11a1*-mCherry targeting construct. SD: Helped in illustrating conceptual diagram. KO: Helped in designing experiments, writing manuscript, critical comments and supervision. DJA: Conducted pulmonary metastasis experiments. JS: Conducted B16-F10 subcutaneous experiments under her PPL and supervised the study. SAT: Supervised the study. All authors commented on and approved of the draft manuscript before submission.

REFERENCES

1 Hanahan, D. & Weinberg, R. A. Hallmarks of cancer: the next generation. *Cell* **144**, 646-674, doi:10.1016/j.cell.2011.02.013 (2011).

2 Miller, W. L. & Auchus, R. J. The molecular biology, biochemistry, and physiology of human steroidogenesis and its disorders. *Endocrine reviews* **32**, 81-151, doi:10.1210/er.2010-0013 (2011).

3 Miller, W. L. Steroidogenesis: Unanswered Questions. *Trends in endocrinology and metabolism: TEM* **28**, 771-793, doi:10.1016/j.tem.2017.09.002 (2017).

4 Belelli, D. & Lambert, J. J. Neurosteroids: endogenous regulators of the GABA(A) receptor. *Nature reviews. Neuroscience* **6**, 565-575, doi:10.1038/nrn1703 (2005).

5 Hosie, A. M., Wilkins, M. E., da Silva, H. M. & Smart, T. G. Endogenous neurosteroids regulate GABAA receptors through two discrete transmembrane sites. *Nature* **444**, 486-489, doi:10.1038/nature05324 (2006).

6 Slominski, A. *et al*. Steroidogenesis in the skin: implications for local immune functions. *The Journal of steroid biochemistry and molecular biology* **137**, 107-123, doi:10.1016/j.jsbmb.2013.02.006 (2013).

7 Vacchio, M. S., Papadopoulos, V. & Ashwell, J. D. Steroid production in the thymus: implications for thymocyte selection. *The Journal of experimental medicine* **179**, 1835-1846 (1994).

8 Li, J., Papadopoulos, V. & Vihma, V. Steroid biosynthesis in adipose tissue. *Steroids* **103**, 89-104, doi:10.1016/j.steroids.2015.03.016 (2015).

9 Cima, I. *et al*. Intestinal epithelial cells synthesize glucocorticoids and regulate T cell activation. *The Journal of experimental medicine* **200**, 1635-1646, doi:10.1084/jem.20031958 (2004).

10 Hostettler, N. *et al*. Local glucocorticoid production in the mouse lung is induced by immune cell stimulation. *Allergy* **67**, 227-234, doi:10.1111/j.1398-9995.2011.02749.x (2012).

11 Cain, D. W. & Cidlowski, J. A. Immune regulation by glucocorticoids. *Nature reviews. Immunology* **17**, 233-247, doi:10.1038/nri.2017.1 (2017).

12 Klein, S. L. & Flanagan, K. L. Sex differences in immune responses. *Nature reviews. Immunology* **16**, 626-638, doi:10.1038/nri.2016.90 (2016).

13 Mahata, B. *et al*. Single-cell RNA sequencing reveals T helper cells synthesizing steroids de novo to contribute to immune homeostasis. *Cell reports* **7**, 1130-1142, doi:10.1016/j.celrep.2014.04.011 (2014).

14 Mellman, I., Coukos, G. & Dranoff, G. Cancer immunotherapy comes of age. *Nature* **480**, 480-489, doi:10.1038/nature10673 (2011).

15 Landskron, G., De la Fuente, M., Thuwajit, P., Thuwajit, C. & Hermoso, M. A. Chronic inflammation and cytokines in the tumor microenvironment. *Journal of immunology research* **2014**, 149185, doi:10.1155/2014/149185 (2014).

16 Papatheodorou, I. *et al*. Expression Atlas: gene and protein expression across multiple studies and organisms. *Nucleic acids research* **46**, D246-D251, doi:10.1093/nar/gkx1158 (2018).

17 Curran, M. A., Montalvo, W., Yagita, H. & Allison, J. P. PD-1 and CTLA-4 combination blockade expands infiltrating T cells and reduces regulatory T and myeloid cells within B16 melanoma tumors. *Proceedings of the National Academy of Sciences of the United States of America* **107**, 4275-4280, doi:10.1073/pnas.0915174107 (2010).

18 De Henau, O. *et al*. Overcoming resistance to checkpoint blockade therapy by targeting PI3Kgamma in myeloid cells. *Nature* **539**, 443-447, doi:10.1038/nature20554 (2016).

19 Zamarin, D. *et al*. Intratumoral modulation of the inducible co-stimulator ICOS by recombinant oncolytic virus promotes systemic anti-tumour immunity. *Nature communications* **8**, 14340, doi:10.1038/ncomms14340 (2017).

20 van der Weyden, L. *et al*. Genome-wide in vivo screen identifies novel host regulators of metastatic colonization. *Nature* **541**, 233-236, doi:10.1038/nature20792 (2017).

21 Skarnes, W. C. *et al*. A conditional knockout resource for the genome-wide study of mouse gene function. *Nature* **474**, 337-342, doi:10.1038/nature10163 (2011).

22 Kranz, A. *et al*. An improved Flp deleter mouse in C57Bl/6 based on Flpo recombinase. *Genesis* **48**, 512-520, doi:10.1002/dvg.20641 (2010).

23 Martinez, F. O. & Gordon, S. The M1 and M2 paradigm of macrophage activation: time for reassessment. *F1000prime reports* **6**, 13, doi:10.12703/P6-13 (2014).

24 Gordon, J. R., Ma, Y., Churchman, L., Gordon, S. A. & Dawicki, W. Regulatory dendritic cells for immunotherapy in immunologic diseases. *Frontiers in immunology* **5**, 7, doi:10.3389/fimmu.2014.00007 (2014).

25 Sakuishi, K. *et al*. Targeting Tim-3 and PD-1 pathways to reverse T cell exhaustion and restore anti-tumor immunity. *The Journal of experimental medicine* **207**, 2187-2194, doi:10.1084/jem.20100643 (2010).

26 Anderson, A. C., Joller, N. & Kuchroo, V. K. Lag-3, Tim-3, and TIGIT: Co-inhibitory Receptors with Specialized Functions in Immune Regulation. *Immunity* **44**, 989-1004, doi:10.1016/j.immuni.2016.05.001 (2016).

27 Chihara, N. *et al*. Induction and transcriptional regulation of the co-inhibitory gene module in T cells. *Nature* **558**, 454-459, doi:10.1038/s41586-018-0206-z (2018).

28 Wiedenheft, B. *et al*. Structures of the RNA-guided surveillance complex from a bacterial immune system. *Nature* **477**, 486-489, doi:10.1038/nature10402 (2011).

29 Hodgkins, A. *et al*. WGE: a CRISPR database for genome engineering. *Bioinformatics* **31**, 3078-3080, doi:10.1093/bioinformatics/btv308 (2015).

30 Pramanik, J. *et al*. Genome-wide analyses reveal the IRE1a-XBP1 pathway promotes T helper cell differentiation by resolving secretory stress and accelerating proliferation. *Genome medicine* **10**, 76, doi:10.1186/s13073-018-0589-3 (2018).

Figure 1

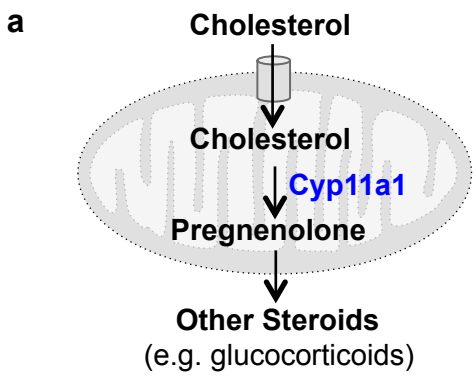
a
Cholesterol
Cholesterol
Cyp11a1
Pregnenolone
Other Steroids
(e.g. glucocorticoids)

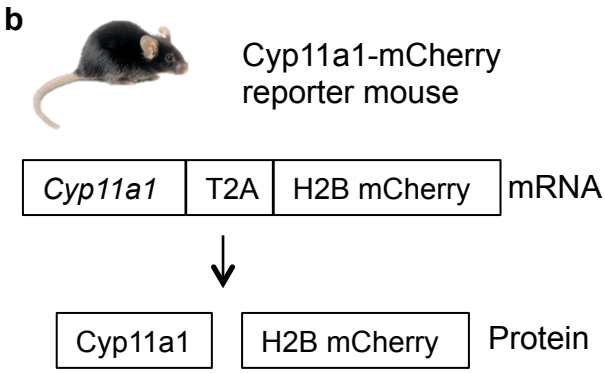
b
Cyp11a1-mCherry
reporter mouse
Cyp11a1
T2A
H2B mCherry
mRNA
Cyp11a1
H2B mCherry
Protein

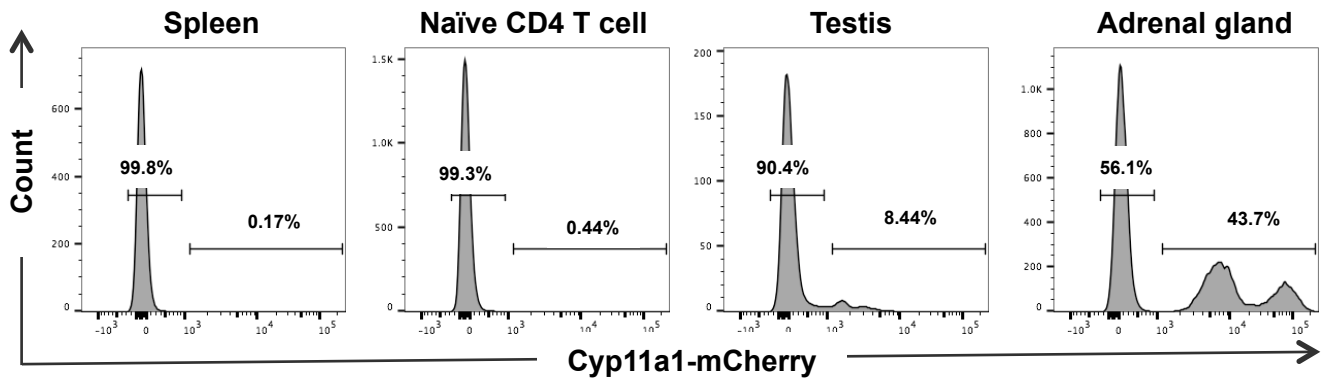
c
Spleen
Naïve CD4 T cell
Testis
Adrenal gland
Count
99.8%
0.17%
99.3%
0.44%
90.4%
8.44%
56.1%
43.7%
Cyp11a1-mCherry

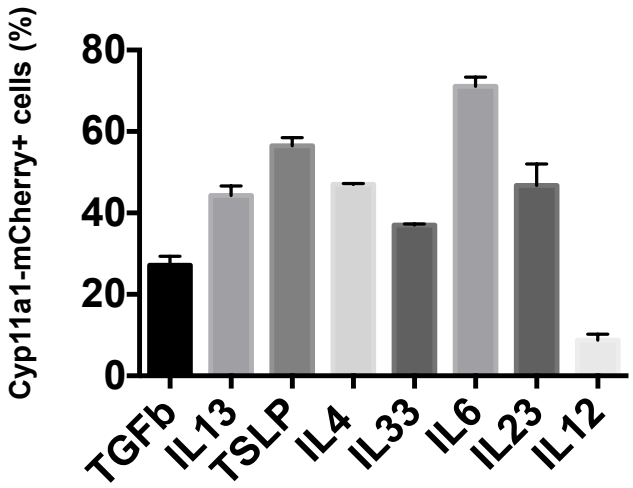
d
Cyp11a1-mCherry+ cells (%)
80
60
40
20
0
TGFb
IL13
TSLP
IL4
IL33
IL6
IL23
IL12

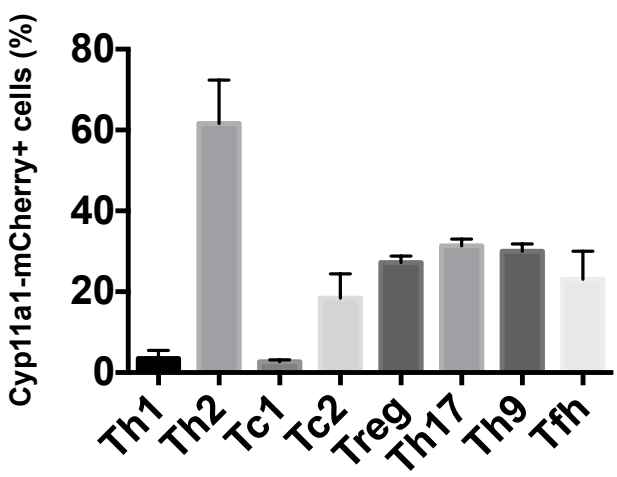
e
Cyp11a1-mCherry+ cells (%)
80
60
40
20
0
Th1
Th2
Tc1
Tc2
Treg
Th17
Th9
Tfh

Figure 1. Generation of a *de novo* steroidogenesis reporter mouse line and its application to steroidogenic T cell analysis

- **a.** Schematic of *de novo* steroidogenesis pathway. In steroidogenic cells, such as testicular Leydig cells, cholesterol is imported into the mitochondria, where CYP11A1 converts it into pregnenolone, the first bioactive steroid of the pathway and precursor of all other steroids. CYP11A1 is the first and a key rate-limiting enzyme of the pathway.
- **b.** *Cyp11a1*-mCherry reporter mice express H2B-tagged mCherry fluorescent protein, and *Cyp11a1* as a single mRNA, driven by the endogenous *Cyp11a1* promoter. The newly synthesized fusion protein self-cleaves due to presence of a T2A peptide and dissociates into two separate proteins: Cyp11a1 and H2B-mCherry.
- **c.** *Cyp11a1*-mCherry reporter mice report Cyp11a1 expression accurately. Spleen, testis and adrenal glands were harvested from *Cyp11a1*-mCherry reporter mice. Tissues were mechanically dissociated and enzymatically digested into single cell suspension. Splenic naïve $CD4^+$ T cells were purified by using anti-CD4 antibody conjugated microbeads by using magnetic activated cell sorting (MACS). Single cell suspensions were analyzed by flow cytometry. Gating: All cells > Singlets > Live cells > Cyp11a1-mCherry. Representative of three independent experiments; each experiment contains 3-4 mice.
- **d.** Induction of Cyp11a1 expression in T cells by cytokines. Splenic naïve $CD4^+$ T cells from *Cyp11a1*-mCherry reporter mice were purified by negative selection; activated in the anti-CD3e and anti-CD28 antibody coated plates in the presence of cytokines for 3 days, rested for 2 days, restimulated 6 hours, and Cyp11a1-mCherry expression was analyzed by flow cytometry. Error bars represent mean ± s.e.m, representative of 3 independent experiments.
- **e.** Cyp11a1 expression in T cells. Splenic naïve $CD4^+$ and $CD8^+$ T cells from *Cyp11a1*-mCherry reporter mice were purified by negative selection; activated in anti-CD3e and anti-CD28 antibody coated plates under Th1, Th2, Th9, Th17, Tfh, Treg, Tc1 and Tc2 differentiation conditions (activation 3 days, resting 2 days), and Cyp11a1-mCherry expression was analyzed by flow cytometry. Error bars represent mean ± s.e.m, representative of 3 independent experiments.

Figure 2

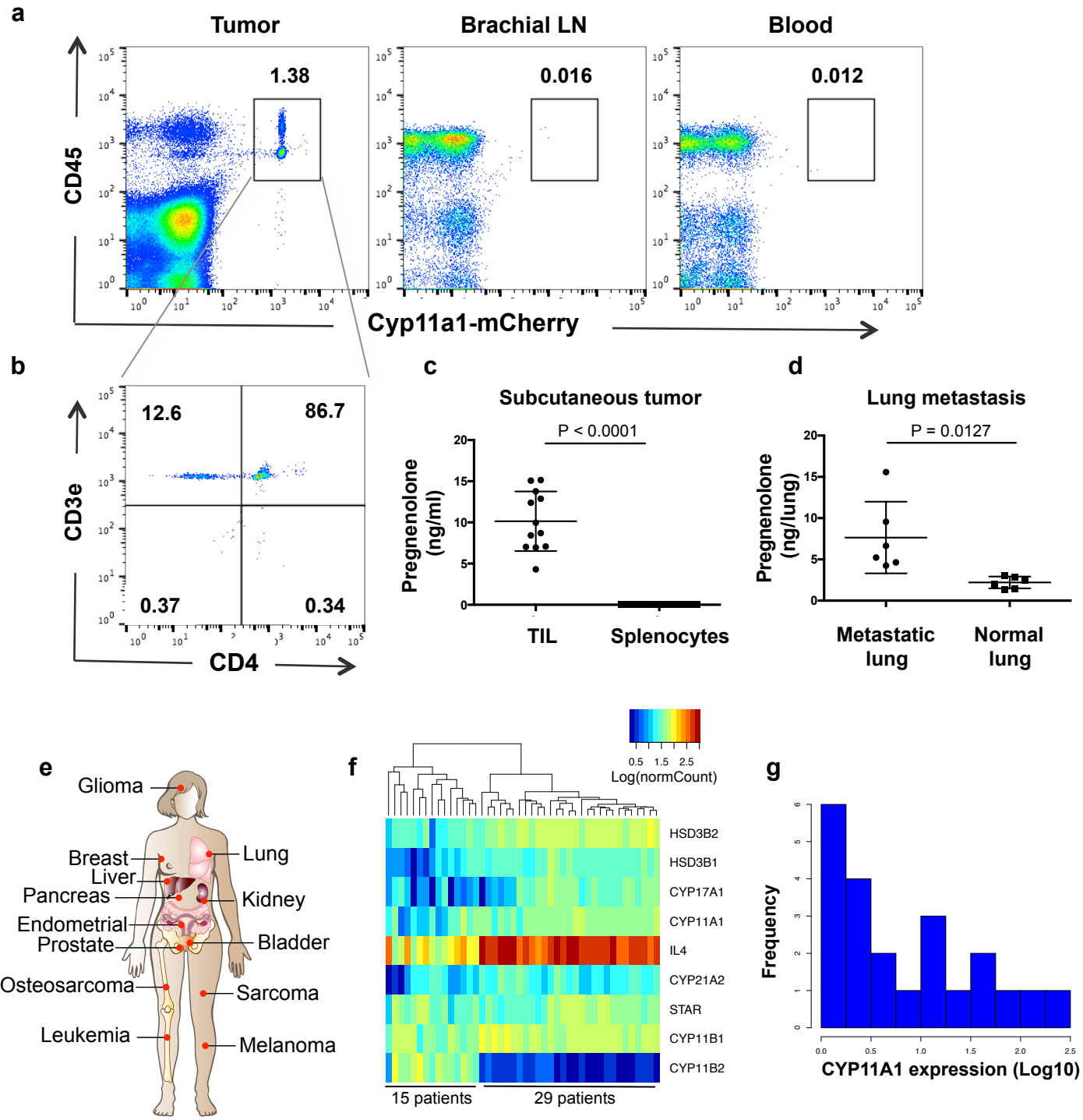
a
Tumor
Brachial LN
Blood
1.38
0.016
0.012
CD45
Cyp11a1-mCherry
b
12.6
86.7
0.37
0.34
CD3e
CD4
c
Subcutaneous tumor
P < 0.0001
Pregnenolone (ng/ml)
TIL
Splenocytes
d
Lung metastasis
P = 0.0127
Pregnenolone (ng/lung)
Metastatic lung
Normal lung
e
Glioma
Breast
Liver
Pancreas
Endometrial
Prostate
Osteosarcoma
Leukemia
Lung
Kidney
Bladder
Sarcoma
Melanoma
f
Log(normCount)
HSD3B2
HSD3B1
CYP17A1
CYP11A1
IL4
CYP21A2
STAR
CYP11B1
CYP11B2
15 patients
29 patients
g
Frequency
CYP11A1 expression (Log10)

Figure 2. Tumors induce steroidogenesis in T cells *in vivo*

- **a.** Presence of steroidogenic (Cyp11a1^{+}) T cells in the B16-F10 melanoma tumor. B16-F10 cells were injected subcutaneously into the shoulder region of *Cyp11a1*-mCherry reporter mice. After 12 days brachial lymph node (LN), blood and tumor tissues were dissociated into single cell suspensions, and analyzed by flow cytometry. Gating strategy: Singlets > Live cells > CD45, Cyp11a1-mCherry. (N=5)
- **b.** Cyp11a1 expression in CD4^{+} T cells. CD45^{+}Cyp11a1-mCherry+ cells were further gated to show T helper cell (CD4^{+}CD3e^{+}) expression of Cyp11a1.
- **c.** TIL supernatant contains pregnenolone. B16-F10 tumor-infiltrating leukocytes (TIL) were purified from tumor-bearing mice on post-inoculation day 12, cultured for 48 hours, and the supernatant was analyzed by ELISA to measure pregnenolone. Splenic leukocytes from the tumor bearing mice were used as control. N=12, pooled analysis of three independent experiments, symbol represents individual mouse, error bars represent mean ± s.e.m., unpaired two-tailed t-test.
- **d.** Metastatic dissemination of cancer cells induces steroid biosynthesis. Metastasized lungs were harvested 10 days post-B16-F10 intravenous injection in C57BL/6 mice, dissociated into single cell suspension, cultured for 48 hours and the supernatant was analyzed by ELISA. Naïve uninfected lungs (normal lung) were used as control. N=6, symbol represents individual mouse, pooled analysis of two independent experiments, error bars represent mean ± s.e.m., unpaired two-tailed t-test.

e-g. Human tumors induce *de novo* steroidogenesis. Publicly available data sets from TCGA, GEO and ArrayExpress were analyzed to identify steroidogenic and cytokine gene expression, and their correlation.

- ***e.*** Human *de novo* steroidogenic tumor types as predicted by *CYP11A1* expression. A diagrammatic presentation of details in Extended Data Figures 3a and b.
- **f.** Steroidogenic gene expression is correlated with *IL4* expression in human melanoma. Hierarchical clustering of steroidogenic genes and *IL4* mRNA expression across 44 melanoma patient samples (Raw data source: GEO: GSE19234).
- **g.** Frequency distribution histogram showing *CYP11A1* mRNA expression (normalized read counts, log10 scale) across 22 melanoma patients' tumor infiltrating CD4^{+} T cells (Raw data accession code EGAD00001000325).

Figure 3

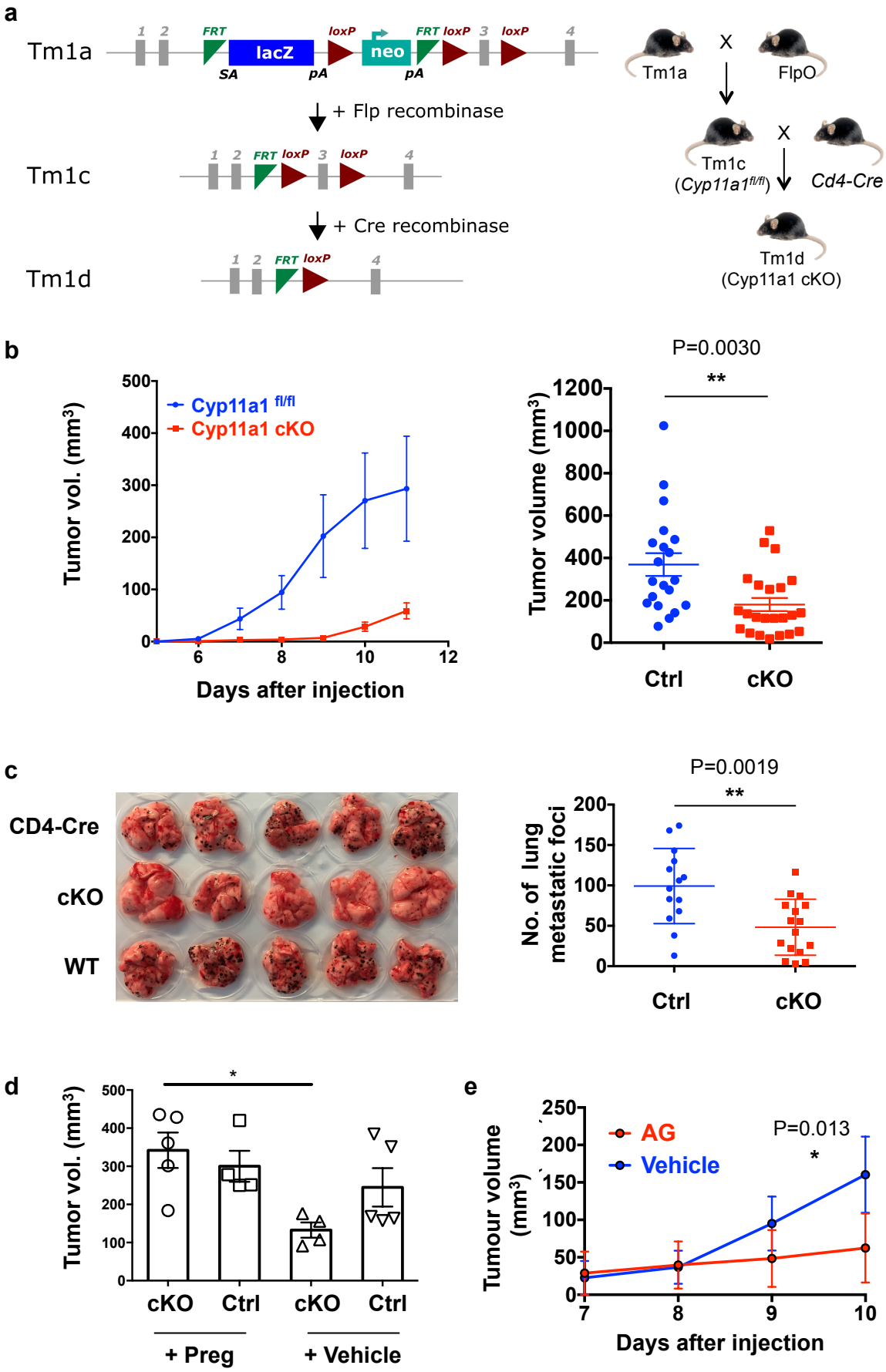
a
Tm1a
1 2 FRT lacZ loxP neo FRT loxP 3 loxP 4
SA pA pA
+ Flp recombinase
Tm1c
1 2 FRT loxP 3 loxP 4
+ Cre recombinase
Tm1d
1 2 FRT loxP 4
Tm1a
X
FlpO
Tm1c
(Cyp11a1fl/fl)
X
Cd4-Cre
Tm1d
(Cyp11a1 cKO)
b
Cyp11a1 fl/fl
Cyp11a1 cKO
Tumor vol. (mm3)
Days after injection
P=0.0030
**
Tumor volume (mm3)
Ctrl
cKO
c
CD4-Cre
cKO
WT
P=0.0019
**
No. of lung metastatic foci
Ctrl
cKO
d
*
Tumor vol. (mm3)
cKO
Ctrl
cKO
Ctrl
+ Preg
+ Vehicle
e
AG
Vehicle
P=0.013
*
Tumour volume (mm3)
Days after injection

Figure 3. Ablation of T cell *de novo* steroidogenesis restricts experimental tumor growth and metastasis

- **a.** Generation of a *Cyp11a1* conditional knockout mice**.** Schematic presentation of the *Cyp11a1* conditional knockout mouse line and generation of T cell specific *Cyp11a1* knockout mice (*Cd4-Cre;Cyp11a1*$^{fl/fl}$). The targeting allele is shown in the left-hand-side panel and the crossing strategy is on the right.
- **b.** Genetic deletion of *Cyp11a1* in T cells inhibits primary tumor growth of B16-F10 melanoma cells. *Left-panel*: B16-F10 subcutaneous tumor growth curve assessed in T cell specific *Cyp11a1* cKO (cKO) and *Cd4*-Cre control mice (n=5, representative of four independent experiments, error bars represent mean ± s.e.m.). Tumors were measured every day from 6th day after subcutaneous injection of B16-F10 cells. *Right panel*: Graphical presentation of end-point tumor volume (n ≥ 20, pooled data of four independent experiments, error bars represent mean ± s.e.m., unpaired two-tailed t-test).
- **c.** Genetic deletion of *Cyp11a1* in T cells inhibits experimental lung metastasis. *Left panel:* Representative photograph of pulmonary metastatic foci produced 10 days after tail vein injection of B16-F10 cells. *Right panel*: Graphical presentation of the numbers of lung metastatic foci (right panel) (n ≥ 15, pooled data of three independent experiments, error bars represent mean ± s.e.m., unpaired two-tailed t-test).
- **d.** Pregnenolone complements the Cyp11a1 deficiency in *Cyp11a1* cKO mice. *Cyp11a1* cKO and *Cd4*-Cre control mice were injected with B16-F10 cells. Pregnenolone or vehicle (DMSO) applied topically at the primary tumor site every 48 hrs. Tumor volume was measured at the end-point at day 12. N=5, error bars represent mean ± s.e.m., one way ANOVA, representative experiment.
- **e.** B16-F10 cells were injected subcutaneously in C57BL/6 mice with or without Cyp11a1 inhibitor aminoglutethimide (AG). AG treatment was continued with a 48 hrs interval (N=5, error bars represent mean ± s.d., two way ANOVA, P=0.013, representative experiment).

Figure 4

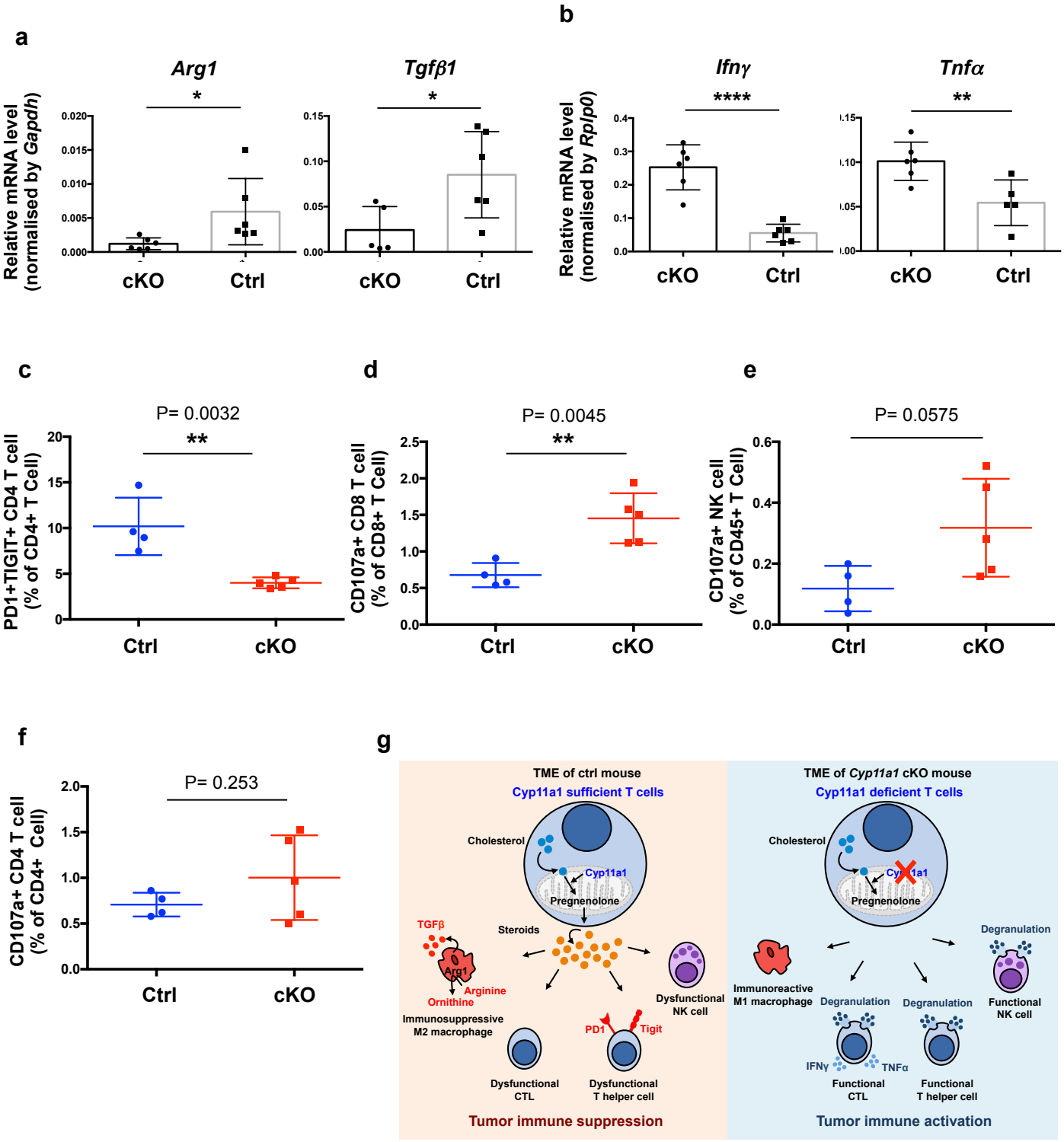
a
Arg1
Tgfβ1
Relative mRNA level (normalised by Gapdh)
*
*
cKO
Ctrl
b
Ifnγ
Tnfα
Relative mRNA level (normalised by Rplp0)
****
**
cKO
Ctrl
c
P= 0.0032
**
PD1+TIGIT+ CD4 T cell (% of CD4+ T Cell)
Ctrl
cKO
d
P= 0.0045
**
CD107a+ CD8 T cell (% of CD8+ T Cell)
Ctrl
cKO
e
P= 0.0575
CD107a+ NK cell (% of CD45+ T Cell)
Ctrl
cKO
f
P= 0.253
CD107a+ CD4 T cell (% of CD4+ Cell)
Ctrl
cKO
g
TME of ctrl mouse
Cyp11a1 sufficient T cells
Cholesterol
Cyp11a1
Pregnenolone
Steroids
TGFβ
Arg1
Arginine
Ornithine
Immunosuppressive M2 macrophage
Dysfunctional NK cell
PD1
Tigit
Dysfunctional CTL
Dysfunctional T helper cell
Tumor immune suppression
TME of Cyp11a1 cKO mouse
Cyp11a1 deficient T cells
Cholesterol
Pregnenolone
Immunoreactive M1 macrophage
Degranulation
Degranulation
Degranulation
Functional NK cell
IFNγ
TNFα
Functional CTL
Functional T helper cell
Tumor immune activation

Figure 4. Inhibition of T cell steroidogenesis boosts anti-tumor immunity. Comparing *Cyp11a1* cKO and *Cd4*-Cre control mice with B16-F10 cells injected subcutaneously (n= 5 or 6, error bars represent mean ± s.e.m., unpaired two-tailed t-test, representative experiment)., representative experiment).

- **a.** Tumor infiltrating macrophages ($Lin^{-}CD11b^{+}$) were purified by cell sorting at day 12. *Arg1* and *Tgfb1* mRNA expression was quantified by RT-qPCR, with mRNA expression level normalized by *Gapdh mRNA* expression.
- **b.** Tumour infiltrating $CD3e^{+}CD8^{+}$ T cells purified by cell sorting at day 12, reactivated *ex vivo,* and *Ifng* and *Tnfa* mRNA expression quantified by RT-qPCR, with mRNA expression level was normalised by *Rplp0* expression.
- **c.** Co-inhibitory cell surface receptor PD1 and TIGIT co-expression on tumor infiltrating $CD4^{+}$ T cells analyzed by flow cytometry after 12 days post B16-F10 inoculation. Gating: All cells > singlets > live cells > $CD4^{+}$ T cell > PD1, TIGIT.
- **d.** Cytotoxic T lymphocyte ($CD8^{+}$ T cell) degranulation assay. CD107a/LAMP1 expression on tumor infiltrating CD8+ T cells was analyzed by flow cytometry after 12 days post-inoculation of B16-F10 cells. Gating: All cells > singlets > live cells > $CD8^{+}$ T cell > CD107a.
- **e.** NK cell degranulation assay by measuring CD107a/LAMP1 expression on tumor infiltrating NK cells. Gating: All cells > singlets > live cells > NK cells > CD107a.
- **f.** $CD4^{+}$ T cell degranulation assay by measuring CD107a/LAMP1 expression on $CD4^{+}$ T cells. Gating: All cells > singlets > live cells > $CD4^{+}$ T cell > CD107a
- **g.** Graphical summary of the panels a-f above. T cell mediated *de novo* steroidogenesis in the tumor microenvironment inhibits anti-tumour immunity, in part by inducing M2 phenotype in macrophages and suppressing T and NK cell function. Genetic deletion of *Cyp11a1* boosts anti-tumor immunity.